Available online at www.sciencedirect.com
ScienceDirect
International Journal of Multiphase Flow 34 (2008) 188–205
International Journal of Multiphase Flow
www.elsevier.com/locate/ijmulflow

Friction relaxation model for fast transient flows application to water hammer in two-phase flow – The WAHA code

Beata Kucienska, Jean-Marie Seynhaeve *, Michel Giot

Mechanical Department, TERM Division, Université catholique de Louvain, Belgium

Received 28 November 2005; received in revised form 5 October 2007

Abstract

The paper deals with the problem of the wall shear stress during rapid transient 1D flows in a piping system caused by water hammers in two-phase flow induced by a fast valve closure. The evolution of the transient wall shear stress is interpreted in terms of two steps. The first step is a sudden and dramatic change of the wall shear stress due to the passage of the pressure wave. The second step is a relaxation process of the shear stress which is modeled from the Extended Irreversible Thermodynamics theory. The friction relaxation model (FRM) presented in the first part of this paper describes both steps of the evolution of the wall shear stress during water hammers. The second part of the paper deals with the application of the FRM model as a closure law in the WAHA code. The main purpose of the WAHA code is to predict various situations relative to single- and two-phase water hammer transients in piping systems. The last part of the paper deals with the simulation of several cases from the UMSICHT databank using the adapted WAHA computer code with the FRM model. The results of these simulations are systematically compared with the experimental data. It is concluded that the new FRM model has a clear effect on water hammer pressure wave damping and on the pressure wave propagation velocity.

Keywords: Water hammer; Two-phase flow; Wall shear stress; Fast transient

1. Introduction

The paper deals with the problem of the wall shear stress magnitude during rapid transient 1D flows in a piping system caused by water hammers in two-phase flow induced by a fast valve closure. The evolution of the transient wall shear stress is interpreted in terms of two steps. The first step is a sudden and dramatic change of the wall shear stress due to the passage of the pressure wave which induces an abrupt change of the radial velocity profile. At this time, the new value of the shear stress is quite higher than the value predicted in steady state. The second step which begins just after the passage of the pressure wave is a relaxation process; here the shear stress decreases, tending more or less slowly to the new steady-state value of the shear stress

* Corresponding author. Tel.: +32 (0)10 47 22 33; fax: +32 (0)10 45 26 92.
E-mail address: jm.seynhaeve@uclouvain.be (J.-M. Seynhaeve).

0301-9322/$ - see front matter © 2007 Elsevier Ltd. All rights reserved.
doi:10.1016/j.ijmultiphaseflow.2007.10.001

corresponding to the new average velocity of the flow. The Extended Irreversible Thermodynamics theory is proposed to model this relaxation process.

The friction relaxation model (FRM) presented in the first part of this paper describes both steps of the evolution of the wall shear stress during water hammers. It enables to take into account the information about the velocity gradient at the wall, which is otherwise not available in a 1D modeling.

The second part of the paper deals with the application and adaptation of the FRM model as a closure law in the WAHA computer code. The WAHA computer code has been developed during the WAHALoads project in the frame of the Fifth European Framework Program. The main purpose of the WAHA code is to predict various situations relative to single- and two-phase water hammer transients in piping systems. The WAHA code can simulate thermal–hydraulic transients with one-dimensional six-equation two-fluid model approximations and calculate the hydraulic forces on the piping system due to water hammers in two-phase flow. Some specific numerical features of the WAHA computer code are also presented in this second part.

In the third part of the paper, a description of the UMSICHT test facility PPP which has been used for water hammer tests inducing bubble condensation is given. The installation has been equipped with a new measurement technology including new wire mesh sensors with thermocouples for the measurement of condensation heat transfer and other innovative transient measurement techniques. From the UMSICHT data bank, some basic data have been chosen as reference cases for validating the WAHA code.

The last part of the paper deals with the simulation of several cases from the UMSICHT databank using the adapted WAHA computer code with the FRM model. The results of these simulations are systematically compared with the experimental data. It is concluded that the adapted WAHA code has the ability to correctly predict water hammers in two-phase flow occurring in a piping system. It is also concluded that the new FRM model has a clear effect on water hammer pressure wave damping and on the pressure wave propagation velocity, but not on the amplitude of the first pressure peak induced by the cavitation water hammer.

2. The friction relaxation model

The comparisons of numerical with experimental results show that the simulations of fast transient flows based on a steady wall friction formula do not give good results. The passage of a water hammer pressure wave has a significant influence on the velocity gradient at the wall, which is not taken into account in the steady-state wall friction models. Therefore the transient friction effect due to a water hammer pressure wave has been modeled by the friction relaxation model (FRM) developed by Kucienska et al. (2002) and Kucienska (2004). The friction relaxation model integrates two steps of the wall shear stress evolution that appears in the pipe during the passage of the pressure wave created by a water hammer due to a fast closure of a valve. These two steps in the wall shear stress evolution were underlined by a 2D axisymmetric simulation performed with the a CFD code for an air flow and are clearly shown in Fig. 1. The problem treated by Fluent® is defined above the diagram of Fig. 1.

2.1. First step: sudden change in the wall shear stress

Considering a given location in the pipe, the sudden change in the wall shear stress appears each time the pressure wave is passing through this location. As expected from the 1D theory, the pressure wave splits the space in two zones where the velocity exhibits a jump in its normal component, the magnitude of which is related to the shock strength. As a consequence, when a planar pressure wave has crossed a given section, the velocity profile is simply shifted by a constant value with no distortion of the velocity profile except close to the wall where the no slip condition prevails. This behavior has been already observed by Vardy and Hang (1991) and Pezzinga (1999). The deformation of the velocity profile due to the passage of the pressure wave in the vicinity of the wall is shown in Fig. 2 for an acceleration of the flow and in Fig. 3 for a deceleration of the flow respectively.

Several simulations with the a CFD code performed for different initial mean velocities of the flow have shown that the amplitude of the sudden change in the wall shear stress at the wall is roughly proportional to the amplitude of the pressure wave. According to the Joukowsky relation, this amplitude is proportional to the mean flow velocity discontinuity between the front and the rear part of the pressure wave:

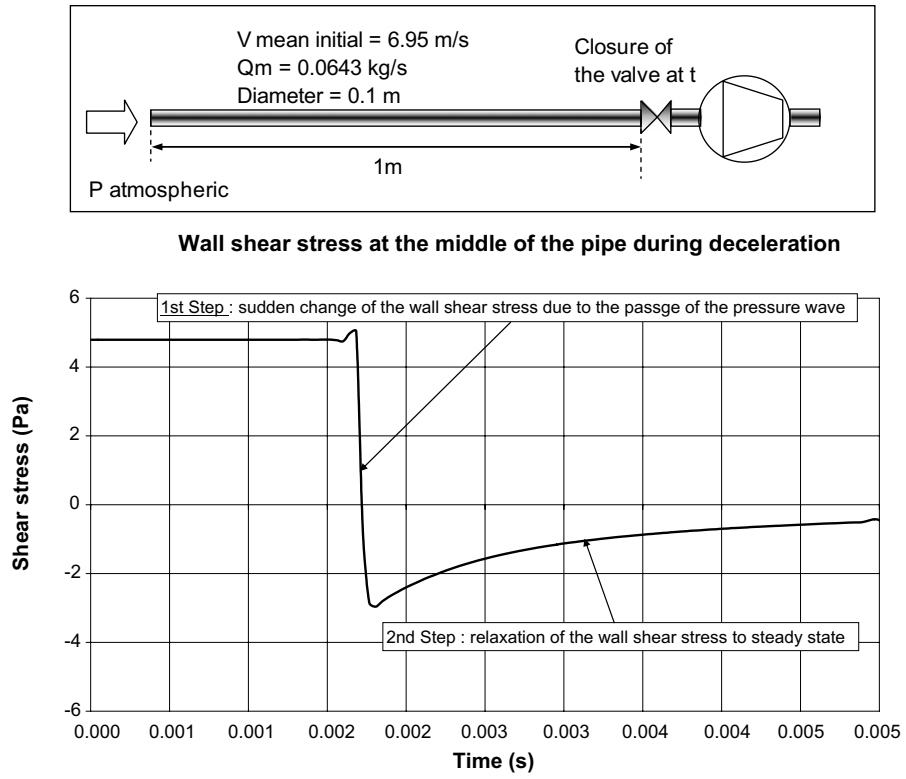

Fig. 1. Wall shear stress evolution predicted by the Fluent® CFD code for the fast transient air flow created by the instantaneous closure of a valve. At the time of the passage of the pressure wave, one notes a sudden reduction of the wall shear stress followed by a progressive recovery.

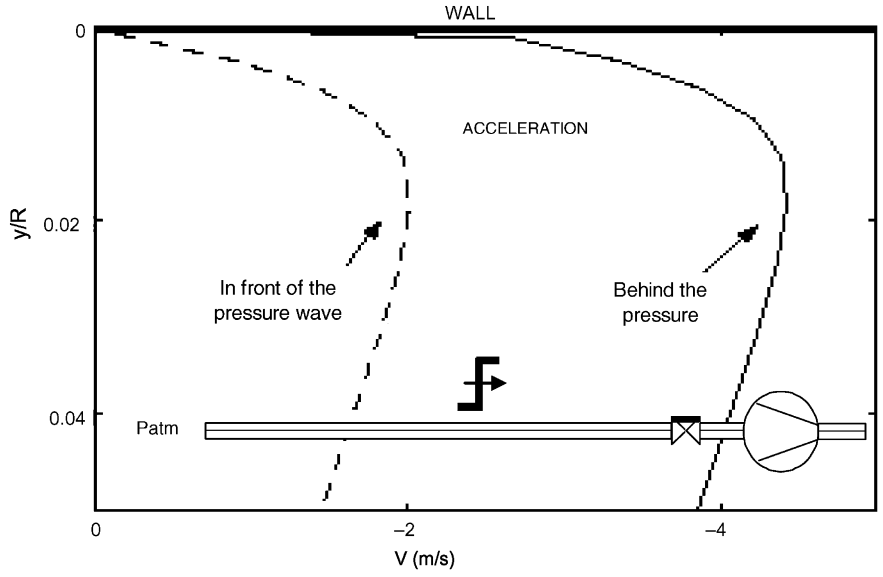

Fig. 2. Deformation of the velocity profile – acceleration.

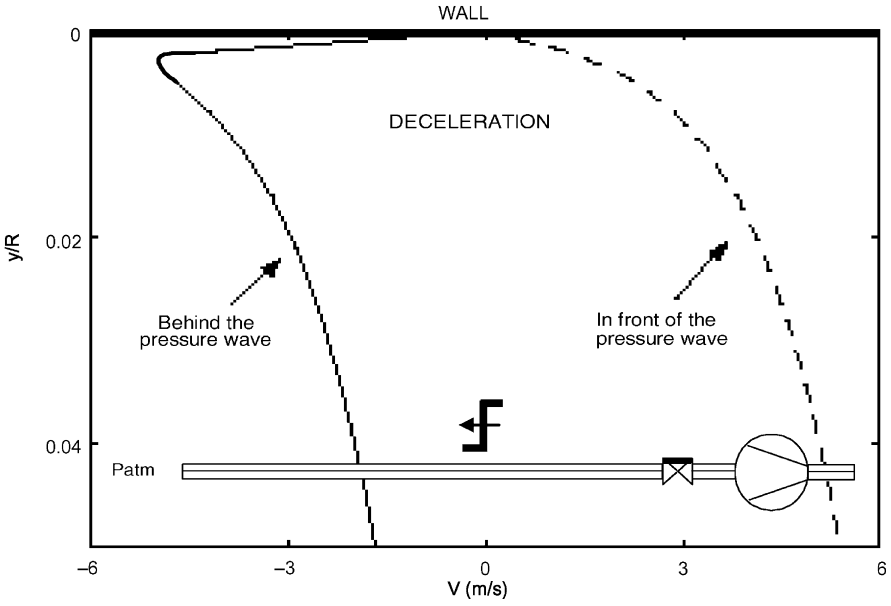

Fig. 3. Deformation of the velocity profile – deceleration.

$$\Delta p_{\text{wave}} = \rho a \Delta v$$

where Δp_{wave} and Δv are the pressure and the velocity change across a shock wave respectively, and a is the isentropic speed of sound. One can thus suggest the following relationship:

$$\Delta\tau = k_T \Delta p_{\text{wave}} = k_T \rho a \Delta v \tag{1}$$

where $\Delta\tau$ is the amplitude of the wall shear stress discontinuity, k_T is a coefficient of proportionality depending on the type of pressure wave (acceleration or deceleration process) and Δv is the mean flow velocity discontinuity. The linear relationship (1) is confirmed by several numerical simulation obtained with Fluent®.

2.2. Second step: relaxation process of the shear stress

Contrary to the first step, the shape of the radial velocity profile is changing continuously during the second step tending to a steady-state profile. The second step is called the "relaxation process" and has been modeled from the Extended Irreversible Thermodynamics (EIT theory (Jou et al., 2001; Bilicki et al., 2002).

EIT postulates the extension of the classical thermodynamic space of variables by variables that reflect the non-equilibrium of the system, such as the dissipative fluxes. In fast transient flows such as water hammers, strong pressure and velocity gradients in space as well as derivatives in time are observed. According to EIT, we can introduce the shear stress as a one-dimensional dissipative flux to the thermodynamic state equation:

$$s = s(u, \rho, \tau^2) \tag{2}$$

where s is the entropy of the system, u the internal energy, ρ the density and τ the wall shear stress (dissipative flux). The square of the shear stress is chosen to ensure a positive value.

Considering Eq. (2), the total derivative of the entropy can be written:

$$\frac{\mathrm{d}s}{\mathrm{d}t} = \left(\frac{\partial s}{\partial u}\right)_{\rho,\tau} \frac{\mathrm{d}u}{\mathrm{d}t} + \left(\frac{\partial s}{\partial \rho}\right)_{u,\tau} \frac{\mathrm{d}\rho}{\mathrm{d}t} + 2\tau \left(\frac{\partial s}{\partial \tau^2}\right)_{\rho,u} \frac{\mathrm{d}\tau}{\mathrm{d}t} \tag{3}$$

We can define the non-equilibrium temperature and pressure from the classical irreversible thermodynamics:

$$\left(\frac{\partial s}{\partial u}\right)_{\rho,\tau} \triangleq \frac{1}{T}$$
$$\left(\frac{\partial s}{\partial \rho}\right)_{u,\tau} \triangleq \frac{p}{\rho^2 T}$$
$$\left(\frac{\partial s}{\partial \rho}\right)_{u,\tau} \triangleq = -\frac{p}{\rho^2 T} \tag{4}$$

Using the mass and energy balance equations for an adiabatic flow and ensuring that the rate of entropy production is positive, we finally obtain the following expression for the wall shear stress during the relaxation process (cf. Kucienska, 2004 and Pezzinga, 1999):

$$\frac{\mathrm{d}\tau}{\mathrm{d}t} = \frac{\tau_s - \tau}{\theta} \tag{5}$$

where τ_s is the wall shear stress corresponding to a fully developed steady-state flow with a mean velocity v and θ is the time constant of the relaxation process to reach steady state conditions.

2.3. The friction relaxation model (FRM)

The friction relaxation model (FRM) integrates the two steps of the wall shear stress evolution explained in Sections 2.1 and 2.2 that appears in the pipe after the passage of the pressure wave:

$$\frac{\mathrm{d}\tau}{\mathrm{d}t} = \frac{\tau_s - \tau}{\theta} + k_T \rho a \frac{\partial v}{\partial t} \tag{6}$$

The second term on the right hand side takes into account the rapid change of the velocity gradient at the wall immediately after the passage of the pressure wave (cf. Section 2.1). The effect on the transient being potentially much larger for liquids than gases, the coefficient k_T has been evaluated on the basis of the Holmboe and Rouleau (1967) water experiment. In this experiment, the water hammer was caused by the fast closure of a downstream valve in a water flow whose initial velocity was 0.244 m/s. The effect of the pipe elasticity has been taken into account. The adjustment of k_T was done in order to obtain the same pressure attenuation as in the experiment, while θ was kept equal to 1.4 ms as for the air flow calculations. The best fit was obtained with $k_T = 2 \times 10^{-4}$ for flow acceleration, and $k_T = 1 \times 10^{-4}$ for flow deceleration. A sensitivity analysis, where the values of k_T were multiplied by a factor of two has shown that the shear stress and to a lesser extent the pressure predictions are sensitive to such variations, but not in a dramatic way. This means that systematic verifications should be performed in the future by using especially designed experiments.

The first term on the right hand side of Eq. (6) represents the relaxation of the wall shear stress associated with the evolution of the velocity profile to the steady-state profile corresponding to the new value of the average velocity behind the pressure wave (cf. 1.2).

The two steps of the evolution of the wall shear-stress are clearly shown in Fig. 4 for several go and back of the pressure wave for the problem posed in Fig. 1. In this figure as well as in Fig. 5, a comparison between the FRM results and the results given by a 2D axisymmetric simulation with Fluent® is also presented. In Fig. 5, the corresponding evolutions of the pressure in the middle of the pipe is shown.

The FRM was also used for predicting the pressure history of a water hammer experiment performed by Simpson (1986). The result of this prediction is given in Fig. 6 and shows a good agreement with the experimental result.

2.4. Approximation of the FRM for code applications

Eq. (6) has a differential form and must be adapted for applying it as a source term in the set of the balance equations used in thermal–hydraulics code.

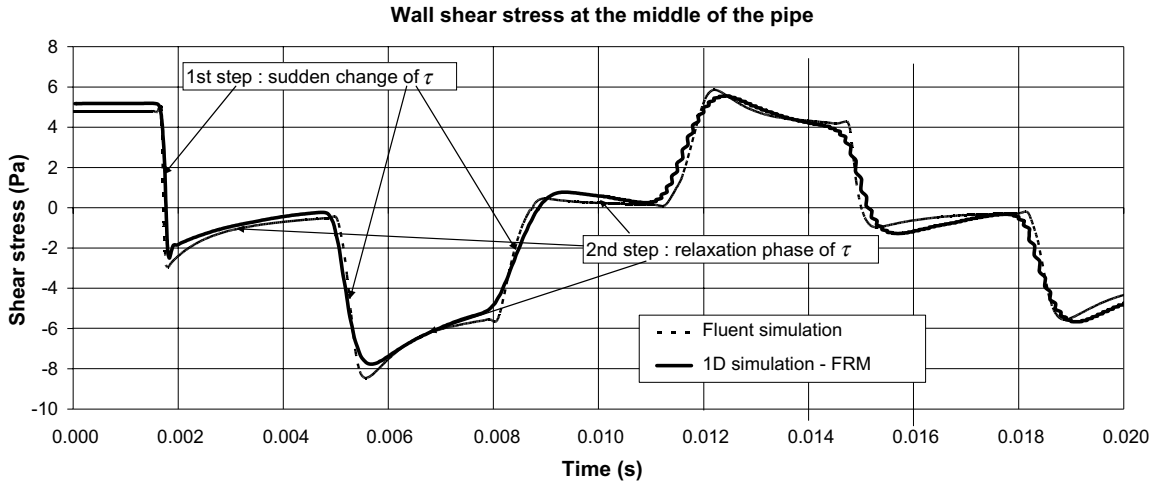

Fig. 4. Comparison between FRM and Fluent® test: wall shear stress at the middle of the pipe (kT: memes valeurs qu'à la Fig. 5 Pourquoi sont-elles différentes de celles annoncées à la page 4).

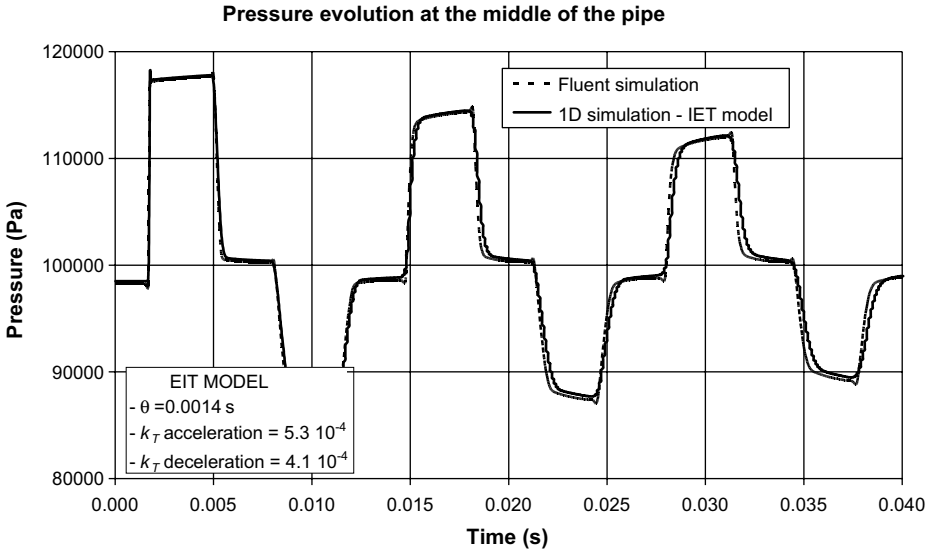

Fig. 5. Comparison between FRM and Fluent® test: pressure at the middle of the pipe.

An approximation of the friction relaxation model was used in the WAHA code. The approximated FRM is a kind of a numerical solution of the exact model expressed by the differential Eq. (6). It is based on the shear stress value obtained at the previous time step during the integration of the set of the differential balance equations:

$$\tau(t) = \tau_s(t) + \tau_{un}(t) \tag{7}$$

with

$$\tau_{un}(t) = \tau_{un}(t - \Delta t)e^{\frac{-\Delta t}{\theta}} + k_T \rho a \Delta v \tag{8}$$

where Δt is the time step chosen for the integration and Δv is the corresponding difference between the successive velocity values. The total shear stress at every time is the sum of the steady shear stress $\tau_s(t)$ and the unsteady contribution $\tau_{un}(t)$ based on its value from the previous time.

At the first time step, we have: $\tau_{un}(0) = 0$.

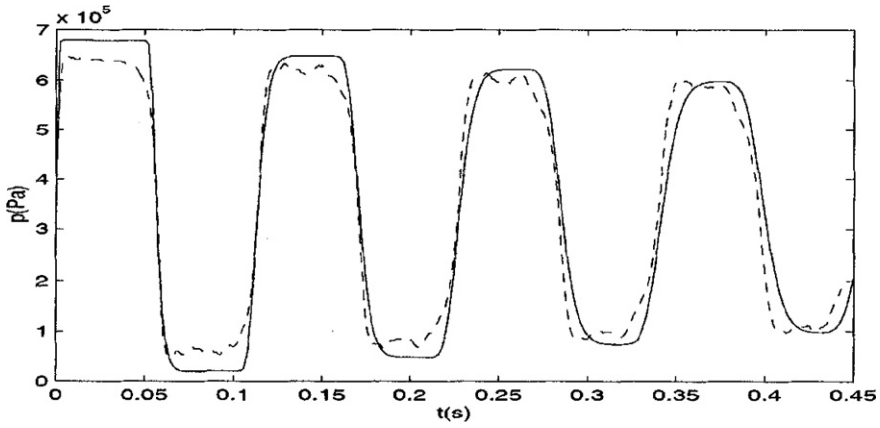

Fig. 6. Pressure history at the valve: Simpson experiment (solid line) – FRM (dashed line).

3. The WAHA code

3.1. Basic equations and models

The six-equation two-fluid model was chosen as a basic mathematical model of WAHA (Tiselj et al., 2004). The simpler five-equation two-fluid model was eliminated because the assumption of vapour being in saturation conditions was found to be too limiting for condensation induced water hammers. The seven-equation two-fluid model with different phase pressures was rejected because of the unknown relations between both pressures. The basic equations are one-dimensional mass, momentum and energy balances for vapour and liquid, without terms for wall-to-fluid heat transfer:

$$\frac{\partial A(1-\alpha)\rho_f}{\partial t}+\frac{\partial A(1-\alpha)\rho_f(v_f-w)}{\partial x}=-A\Gamma_g, \tag{9}$$

$$\frac{\partial A\alpha\rho_g}{\partial t}+\frac{\partial A\alpha\rho_g(v_g-w)}{\partial x}=A\Gamma_g, \tag{10}$$

$$\begin{aligned}&\frac{\partial A(1-\alpha)\rho_f v_f}{\partial t}+\frac{\partial A(1-\alpha)\rho_f v_f(v_f-w)}{\partial x}+A(1-\alpha)\frac{\partial p}{\partial x}-A\cdot\mathrm{CVM}-Ap_i\frac{\partial\alpha}{\partial x}\\&\quad=AC_i|v_r|v_r-A\Gamma_g v_i+A(1-\alpha)\rho_f g\cos\theta-AF_{f,wall},\end{aligned} \tag{11}$$

$$\begin{aligned}&\frac{\partial A\alpha\rho_g v_g}{\partial t}+\frac{\partial A\alpha\rho_g v_g(v_g-w)}{\partial x}+A\alpha\frac{\partial p}{\partial x}+A\cdot\mathrm{CVM}+Ap_i\frac{\partial\alpha}{\partial x}\\&\quad=-AC_i|v_r|v_r+A\Gamma_g v_i+A\alpha\rho_g g\cos\theta-AF_{g,wall},\end{aligned} \tag{12}$$

$$\begin{aligned}&\frac{\partial A(1-\alpha)\rho_f e_f}{\partial t}+\frac{\partial A(1-\alpha)\rho_f e_f(v_f-w)}{\partial x}+p\frac{\partial A(1-\alpha)}{\partial t}+\frac{\partial A(1-\alpha)p(v_f-w)}{\partial x}\\&\quad=AQ_{if}-A\Gamma_g(h_f+v_f^2/2)+A(1-\alpha)\rho_f v_f g\cos\theta,\end{aligned} \tag{13}$$

$$\frac{\partial A\alpha\rho_g e_g}{\partial t}+\frac{\partial A\alpha\rho_g e_g(v_g-w)}{\partial x}+p\frac{\partial A\alpha}{\partial t}+\frac{\partial A\alpha p(v_g-w)}{\partial x}=AQ_{ig}+A\Gamma_g(h_g+v_g^2/2)+A\alpha\rho_g v_g g\cos\theta, \tag{14}$$

Standard notations are used in the above equations: p denotes the pressure, α the vapour volume fraction, v the velocity, w the axial velocity of the pipe, e the specific total internal energy, ρ the density, C_i the interface drag coefficient, θ the inclination of the pipe, v_i the velocity of the interface, Γ_g the vapour generation term, h the specific enthalpy, Q_{if}, Q_{ig} the heat fluxes from interface to phase f or g, and one uses subscripts f for liquid and g for vapour (where p_i is defined and discussed at Eq. (18)). Differential terms are collected on

the left-hand side of the equations and the non-differential terms are collected on the right. Pipe cross-section A can vary as a function of coordinate x and time t:

$$A(x,t) = A(x) + A_e(p(x,t)),$$
$$\frac{dA_e}{A(x)} = \frac{D}{d}\frac{dp}{E} = K\,dp \tag{15}$$

The A_e term takes into account the elasticity of the pipe walls (E is the pipe elasticity modulus, D the pipe diameter, and d the pipe wall thickness), which modifies the propagation velocities in the elastic pipes and is especially important when modelling water hammer transients. The exact value of K depends on the boundary condition on the outer shell of the pipe, and has to be adjusted to the particular conditions under consideration. Here we assume that the pipe wall is free to move radially.

3.2. Additional closure laws

Additional closure equations are needed to close the set of Eqs. (9)–(14).

1. The equation of state for phase k is:

$$d\rho_k = \left(\frac{\partial \rho_k}{\partial p}\right)_{u_k} dp + \left(\frac{\partial \rho_k}{\partial u_k}\right)_{p} du_k \tag{16}$$

   Derivatives on the right hand side of Eq. (16) are determined by the water property subroutines developed for the WAHA code using pressure and temperature (T) or specific internal energy (u) as input. Properties – including metastable states – are interpolated from the pre-tabulated data at 400 pressures (0–1000 bar) and 475 temperatures (273.15–1638 K). These data are calculated by the thermodynamic property correlations of Haar et al. (1984).
2. The virtual mass term CVM in Eqs. (11) and (12) is used to achieve hyperbolicity of the equations in dispersed flow:

$$\mathrm{CVM} = (1-S)C_{vm}\alpha(1-\alpha)\rho_m\left(\frac{\partial v_g}{\partial t} + v_f\frac{\partial v_g}{\partial x} - \frac{\partial v_f}{\partial t} - v_g\frac{\partial v_f}{\partial x}\right) \tag{17}$$

   The value of coefficient C_{vm} was tuned to ensure the hyperbolicity of the two-fluid model equations (Tiselj and Petelin, 1997). Note that the applied virtual mass term does not ensure unconditional hyperbolicity of the equations: for very large relative velocities (comparable to the sonic velocity) complex eigenvalues may appear. However this did not happen for any of the physical test cases used during the WAHA code development. The S factor is taken as $S = 0$ for dispersed flow, $S = 1$ for horizontally stratified flow, and $0 < S < 1$ for transitional flow (Tiselj et al., 2004).
   This factor enables to describe the surface waves in horizontally stratified flows.
3. The interfacial pressure term exists only in stratified flow:

$$p_i = S\alpha(1-\alpha)(\rho_f - \rho_g)gD \tag{18}$$

   where S represents the stratification factor as already mentioned in point 2.
4. The WAHA code distinguishes two flow regimes: the dispersed flow and the horizontally stratified flow, with a transition area between both regimes. The source terms are flow regime dependent and their detailed form is given in the WAHA manual (Tiselj et al., 2004). The terms that do not include derivatives – source terms – are:
   - Terms with C_i – inter-phase drag.
   - Terms with Γ_g, Q_{ig}, Q_{if} – inter-phase exchange of mass and energy.
   - Terms due to the variable pipe cross-section.
   - Terms due to wall friction F_f and F_g.
   - Term with $g\cos\theta$ – volumetric forces.
   - Terms for wall-to-fluid heat, mass, and momentum transfers are neglected in the WAHA code.

The coefficients which appear in the heat, mass, and momentum transfer correlations for horizontally stratified flows are derived from "standard" (Mills, 1999) correlations for a flow near a flat wall. The heat and mass transfer model for dispersed flow is derived from the Homogeneous Relaxation Model (Downar-Zapolski et al., 1996; Lemmonier, 2002), with the additional assumption of a very large gas-interface heat transfer coefficient for the vapour. The inter-phase drag for dispersed flows is modelled with correlations valid for bubbly and droplet flows. The criterion for the transition from horizontally stratified to dispersed flow is based on the onset of the Kelvin–Helmholtz instability.

The axial velocity of the structure w in Eqs. (9)–(14) is set to zero in the current version of the WAHA code and is foreseen for a possible upgrade of the WAHA code into the fluid–structure-interaction code.

3.3. Numerical scheme in WAHA code

The numerical scheme of the WAHA code is based on Godunov characteristic upwind methods. These methods produce solutions with a substantially reduced numerical diffusion and allow the accurate modelling of flow discontinuities. Eqs. (9)–(14) can be written in a vectorial form as:

$$\mathbf{A}\frac{\partial\vec{\psi}}{\partial t}+\mathbf{B}\frac{\partial\vec{\psi}}{\partial x}=\vec{S} \tag{19}$$

where $\vec{\psi}=(p,\alpha,v_{\mathrm{f}},v_{\mathrm{g}},u_{\mathrm{f}},u_{\mathrm{g}})$ represents the vector of the independent variables, matrices $\underline{\mathbf{A}}$ and $\underline{\mathbf{B}}$ represent matrices in front of derivatives of $\vec{\psi}$, and $\vec{S}$ the vector of sources. WAHA solves the basic equations in a non-conservative form. Numerous tests were performed with the six-equation model (described by Tiselj and Petelin, 1997) with different basic variables, and the most successful set of variables turned out to be $\vec{\psi}=(p,\alpha,v_{\mathrm{f}},v_{\mathrm{g}},u_{\mathrm{f}},u_{\mathrm{g}})$.

Non-conservative variables present an acceptable approximation for fast transients while for the long transients, where conservation of mass and energy is more important, this might be a drawback. In the test calculations reported in the WAHA code manual (Tiselj et al., 2004), negligible fluctuations of the overall mass and energy have been observed despite the non-conservative scheme.

Due to the stiffness of the relaxation (inter-phase exchange) source terms, the WAHA code uses a two-step operator splitting to solve Eq. (19):

1st Step: Convection and non-relaxation source terms – source terms due to the smooth area change, wall friction and volumetric forces – are solved in the first sub step:

$$\mathbf{A}\frac{\partial\vec{\psi}}{\partial t}+\mathbf{B}\frac{\partial\vec{\psi}}{\partial x}=\vec{S}_{\mathrm{NON\_RELAXATION}} \tag{20}$$

Eq. (20) is solved with a characteristic upwind numerical scheme, which is based on the explicit evaluation of the eigenvalues of the Jacobian matrix $\mathbf{C}=\mathbf{A}^{-1}\mathbf{B}$ of the system:

$$\mathbf{C}=\mathbf{L}\cdot\mathbf{\Lambda}\cdot\mathbf{L}^{-1} \tag{21}$$

The diagonal matrix $\mathbf{\Lambda}$ is the matrix of eigenvalues and $\mathbf{L}$ is the matrix of eigenvectors of matrix $\mathbf{C}$. The eigenvalues, the eigenvectors, and the inverse matrix of the eigenvectors are numerically calculated between the grid points in the WAHA code. An upwind discretisation of the spatial derivatives is then performed in the space of the characteristic variables. A second-order accurate scheme is obtained with implementation of the slope limiters. The upwind discretisation and the slope limiters are used also for the calculation of the non-relaxation source terms in Eq. (20) (Tiselj et al., 2004). Such approach preserves the steady-state solutions-for example, steady flow in ducts with a variable cross-section, or steady-state flows in vertical pipes with presence of gravity.

2nd Step: The relaxation source terms are integrated in the second sub-step of the operator splitting method:

$$\mathbf{A}\frac{\mathrm{d}\vec{\psi}}{\mathrm{d}t}=\vec{S}_{\mathrm{RELAXATION}} \tag{22}$$

The relaxation source terms-inter-phase heat, mass and momentum exchange terms-are stiff, i.e., their characteristic time scales can be much shorter than the time scales of the hyperbolic part of the equations. The integration of the relaxation sources within the operator-splitting scheme is performed with variable time steps, which depend on the stiffness of the source terms. The properties of the operator splitting used in the WAHA code are described by Tiselj and Horvat (2002).

4. UMSICHT water hammer experiments

In the frame of the WAHALoads project, the UMSICHT test facility PPP (Dudlik, 2003) has been extended and improved with the installation of a new measurement technology including new wire mesh sensors for local void fraction measurement with thermocouples for the measurement of condensation heat transfer and other innovative transient measurement techniques. This instrumentation was installed in PPP additionally to the existing one. A schematic view and a picture of the test facility PPP are given in Figs. 7 and 8, respectively.

Two different scenarios of water and "cavitation" hammers which are typical of conditions in power plants were investigated on the PPP test facility:

Scenario 1: Water and "cavitation" hammers at increasing temperature (20–180 °C) and at two operating pressures of 1 and 10 bars as shown in Fig. 9.

Scenario 2: Condensation hammer induced by cold water injection in steam as shown in Fig. 10.

The typical scenario 1 for the origin of pressure surges is fast closing valves triggered by the breakdown of auxiliary power and fast acting control devices. For experiments according to scenario 1 the experimental set-up including the main measuring positions is given in Fig. 7.

Hot water is pumped into the circuit from the pressurised vessel B2 into the test pipe section of 110 mm (or 50 mm) inner diameter. When the valve is closed rapidly (while the pump keeps running), pressure waves are induced downstream of the valve in the whole pipe system and measured by fast pressure transducers (P03–P23). Forces on pipe supports are also measured as well as displacements. The measuring frequency is 2 kHz. Local void fraction and temperature distributions in several cross sections of the pipe were measured with a new wire mesh sensor and local void probes (WM) developed by the Forschungszentrum Rossendorf e.V. (FZR).

The operating conditions of the initial steady-state flow of the experiments achieved in the frame of scenario 1 are given in Table 1:

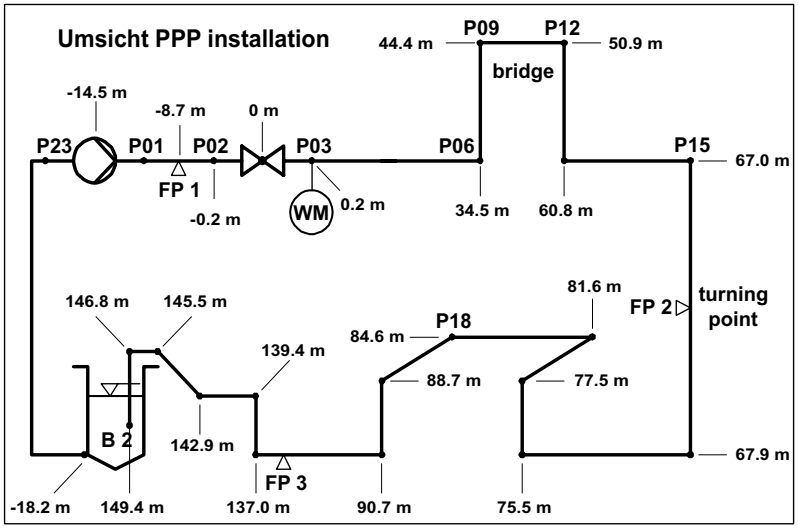

Fig. 7. Sketch of the PPP facility in UMSICHT (P = pressure measurement; WM = wire mesh sensor; FP = fixed point).

Fig. 8. Picture of the PPP facility in UMSICHT.

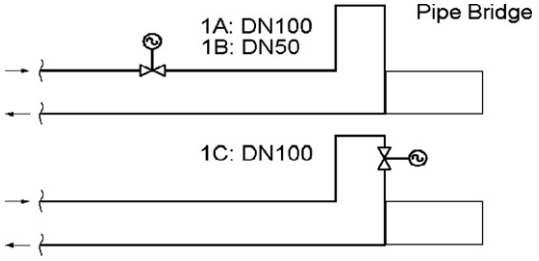

Fig. 9. PPP experiment: scenario 1: sudden closure of the valve. Observation of the phenomenon in the downstream section of the pipe.

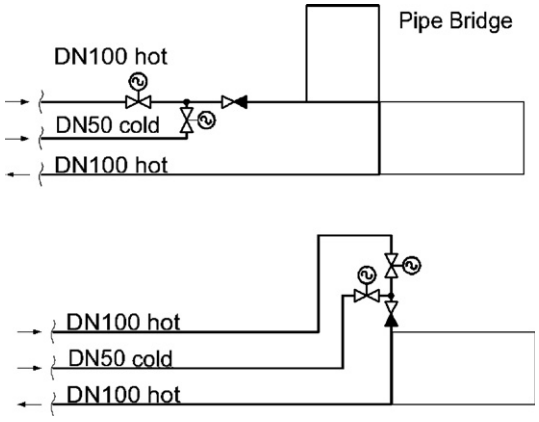

Fig. 10. PPP experiment: scenario 2: closure of the main pipe followed by a cold water injection downstream of the valve.

In this paper, the reference test of the PPP experiments which has been selected for the comparison with the WAHA code simulation is test No. 307. For this test, the following initial conditions at the starting of the fast closure of the valve have been measured:

Table 1
PPP experiment characteristics – scenario 1

Initial steady state velocity	$1.0 \leqslant v \leqslant 5$ m/s	5 velocities
Liquid temperature	$20 \leqslant \vartheta \leqslant 150$ °C	9 temperatures
Re-opening of valve after 10 s	Yes/ no	–
System pressure	1.0; 10 bar	2 pressures

- Pressure in the B2 tank: 9.92 bar.
- Initial water temperature: 119.1 °C.
- Initial water flow rate: 132.2 m^3/h.
- Mean water velocity of about 4 m/s.

The experimental data of this test, i.e. pressure and void fraction evolution close to the valve, are given in Section 4 below.

5. WAHA code simulations

Three particular test cases have been selected for testing the ability of the WAHA code to correctly predict fast transient two-phase flows in different situations:

- Super Moby Dick experiment – steady state critical two-phase flow.
- Benchmark simulations of "cavitation" water hammer with the FRM model.
- PPP water hammer tests – depressurisation inducing cavitation water hammer initiated by a fast valve closure.

For each of these particular test cases, a systematic comparison between the data and the results of the WAHA code are given below. Several possible options of the WAHA code corresponding to different models have also been tested.

5.1. Super moby dick experiment

The Super Moby Dick tests were chosen for verifying the ability of the WAHA code to correctly reproduce steady state situations, for example critical two-phase flows.

The Super Moby Dick experiments performed by the CEA Grenoble (Rousseau, 1986) consist in two-phase critical flashing flow experiments. Steady-state critical flow conditions were measured in a long nozzle. The nozzle has a convergent section at the entrance followed by a straight pipe of about 0.5 m long and of 20 mm inner diameter and ended by a 7° divergent section.

For the WAHA code simulation, the pipe is initially filled with pure liquid at the inlet pressure and inlet temperature of the test. The liquid is at rest (velocity equal to zero). The transient is initiated by imposing the pressure at the outlet of the nozzle corresponding to the pressure measured during the test. The simulation is run until a steady-state critical flow is established.

Two Super Moby Dick tests have been chosen for the comparison with the WAHA code simulations. The inlet conditions of these tests are:

– test 1: Inlet pressure of 20 bar, inlet temperature of 192.3 °C.
– test 2: Inlet pressure of 120 bar, inlet temperature of 305.7 °C.

The back pressure, located at the downstream end of the divergent nozzle, is the atmospheric pressure.

The pressure profiles in the convergent and in the straight pipe predicted by the WAHA code for the two tests and the pressure measurements are given in Figs. 11 and 12.

Since the Homogeneous Relaxation Model (Downar-Zapolski et al., 1996) was developed by using the Super Moby Dick experimental results, and used in the WAHA code in its basic option, the agreement

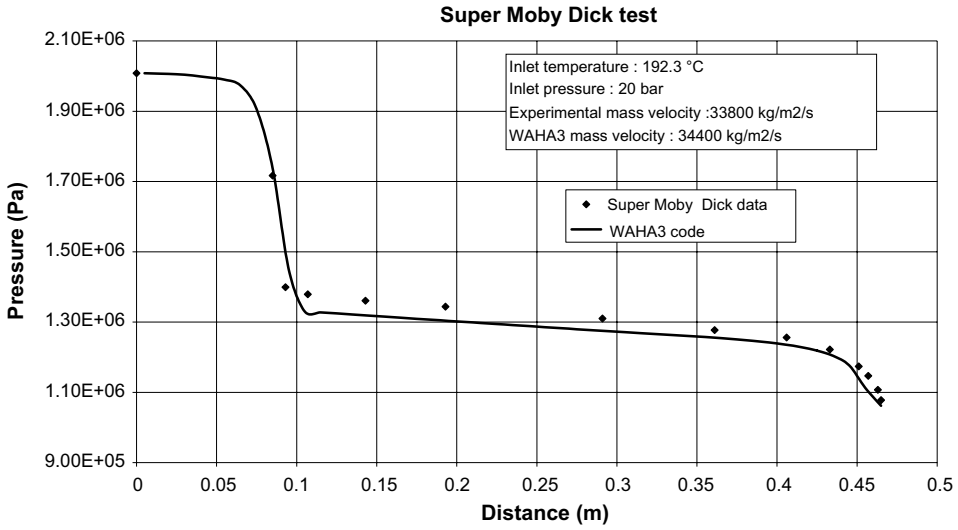

Fig. 11. Super Moby Dick: test 1.

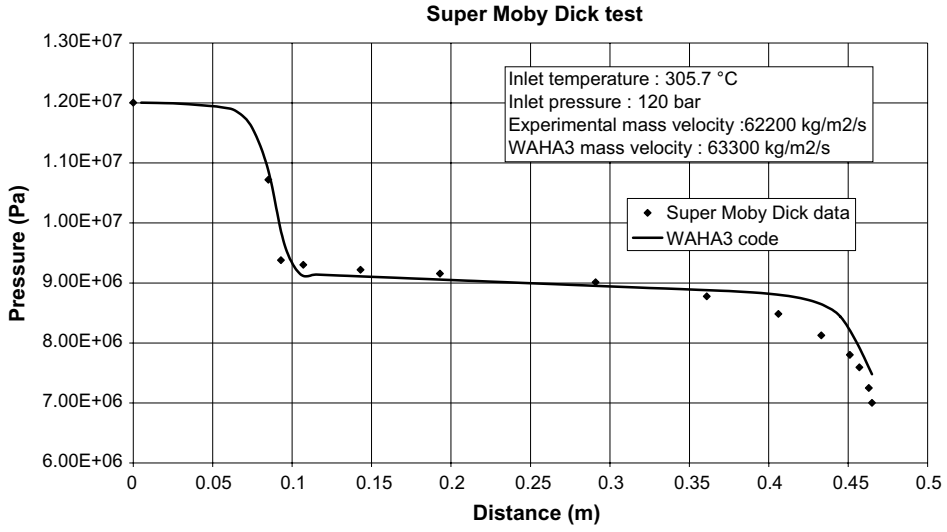

Fig. 12. Super Moby Dick: test 2.

between the WAHA code simulations and the experimental data is excellent. Measured and predicted mass flow velocities are very close to each other too.

5.2. Benchmark test with FRM model

In order to show the impact of the friction relaxation model on the "cavitation" water hammer, benchmark case 1 proposed during the WAHALoads project has been chosen as the reference case. The cavitation water hammer was induced by the fast closure of a valve placed downstream from a straight pipe. The characteristics of the pipe are as followed:

- Diameter: 20 mm
- Length: 50 m

– Initial velocity: 5 m/s
– Initial temperature: 523 K

The results of the WAHA code simulations with the FRM and with the "steady state" wall shear stress model are given in Figs. 13 and 14 where the pressure and the void fraction evolutions at the middle of the pipe are given for both cases. As observed in Fig. 14, the FRM does not have much influence on the quantity of vapor created at the middle of the pipe. On the other hand, the evaporation starts later for the FRM compared with the "steady state" wall friction model, especially for the second flashing. This result has to be related to the result of Fig. 13 where we can clearly observe a phase shift between both pressure evolutions. This means that the friction relaxation model influences the pressure wave propagation velocity.

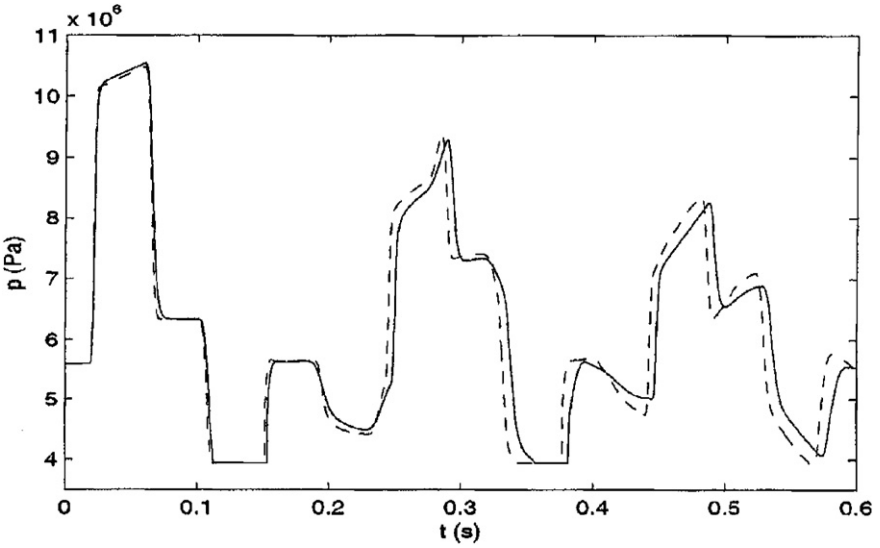

Fig. 13. Pressure evolution at the middle of the pipe: FRM: solid line–dashed line: "Steady state" model.

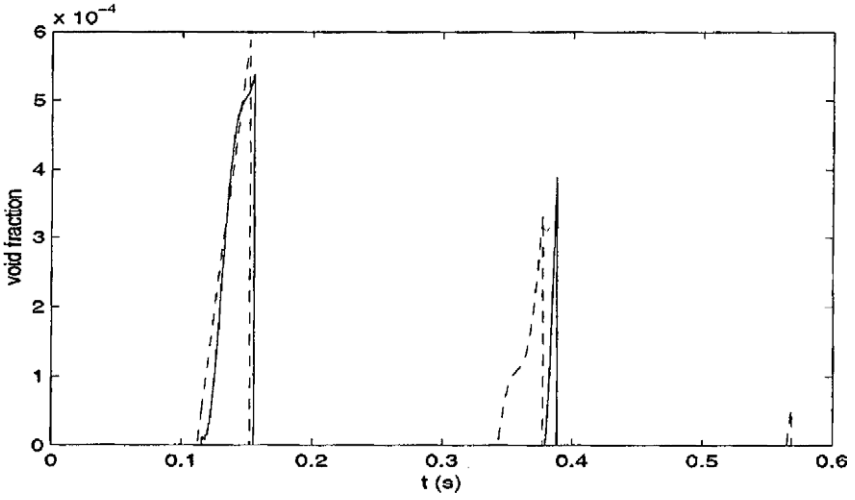

Fig. 14. Void fraction evolution at the middle of the pipe: FRM: solid line–dashed line: "Steady state" model.

5.3. UMSICHT tests

For the PPP facility described in Section 3, one transient experiment (test 307) corresponding to scenario 1-cavitation water hammer due to the fast closure of a valve-has been selected for the comparison with the WAHA code simulations.

Different options of the WAHA code have been tested for this test case:

- Homogeneous relaxation model (HRM) with steady state wall friction model.
- Homogeneous equilibrium model (HEM) with steady state wall friction model.
- Homogeneous relaxation model (HRM) with the friction relaxation model (FRM).

Before simulating the transient due to the fast closure of the valve, the steady state flow conditions need to be reproduced all along the pipe system. These conditions have been determined with the WAHA code with the following boundary conditions:

- Pressure in the downstream tank: 9.92 bar.
- Inlet water temperature: 119.1 °C.
- Mean water velocity at the entrance of the pipe (at the valve location): 4.01 m/s.

The pressure profile along the pipe after 10 s of simulation is given in Fig. 15. We can observe on this figure that the steady state conditions of the flow are obtained after this time.

These conditions have been chosen as the initial flow conditions for the test case simulating the transient after the closure of the valve. To simulate this second step of the test case, the restart option of the WAHA code was used to automatically create the adequate input file. Only the boundary condition corresponding to constant velocity at the entrance has been replaced by a close end condition.

The pressure evolution during the transient just downstream the valve (pressure P03) predicted by the WAHA code is given in Fig. 16 in comparison with the experimental data. The void fraction is shown in Fig. 17.

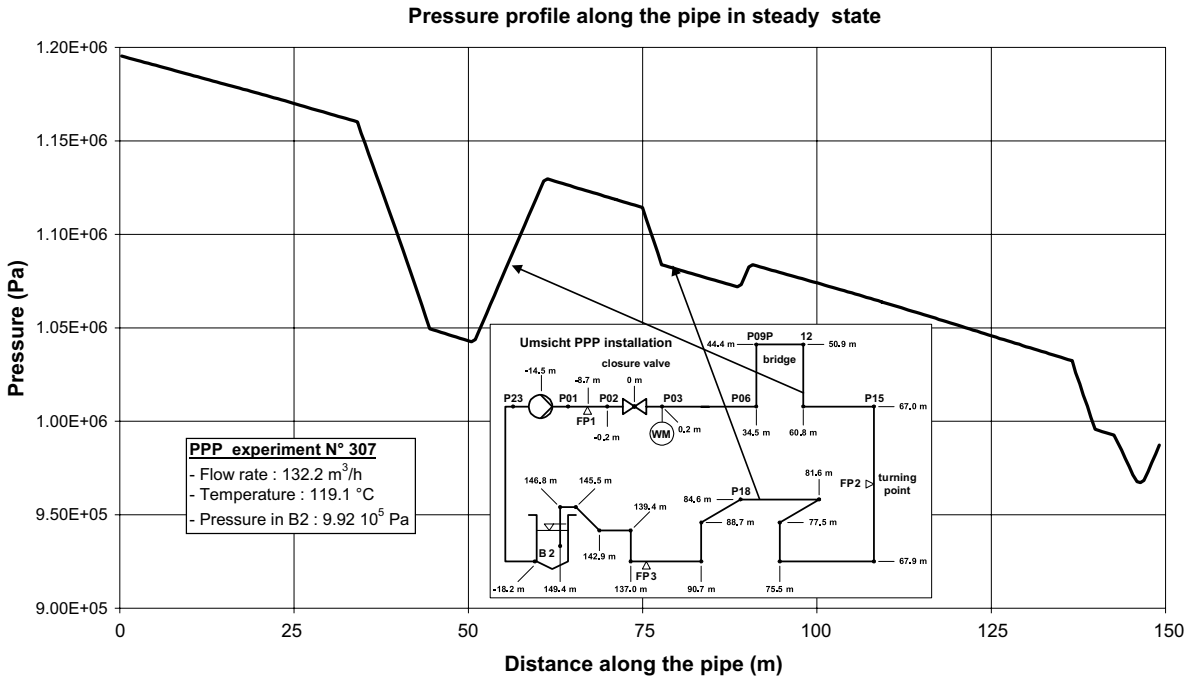

Fig. 15. Steady state conditions for UMSICHT test 307.

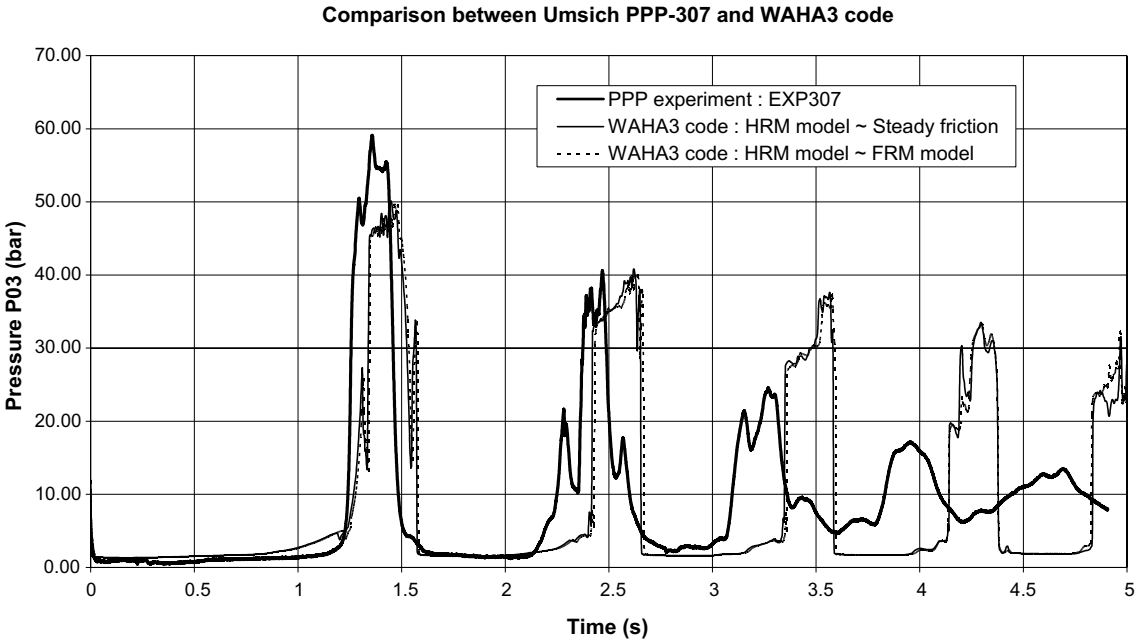

Fig. 16. Test 307: pressure history near the valve.

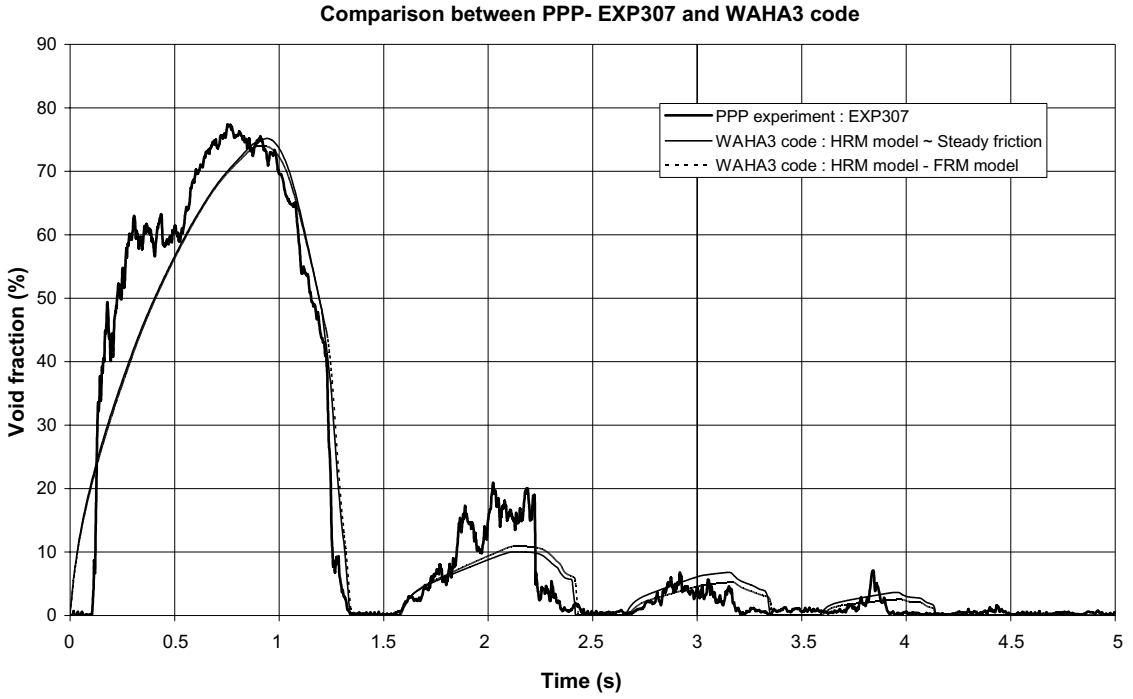

Fig. 17. Test 307: void fraction history near the valve.

We can observe that the first pressure peak occurs much later than the time needed for one go and back of the pressure wave at the speed of sound of the liquid (about 1500 m/s). This can be explained by the additional time needed to condense the steam pocket created near the valve just after its closure. The time for condensing

the steam depends on the speed of sound in two-phase flow which is much less than the speed of sound in liquid. The water hammer occurs just after this condensing process.

We can conclude that:

- The WAHA code can more or less correctly predict the first pressure surge due to the cavitation water hammer. For this first peak, there is no big difference between the models: HRM, HEM, FRM.
- The pressure surges following the first peak are not well predicted neither for the peak amplitude nor the peak phase. However, the HRM model is much better than the HEM model which means that the mass and energy transfer plays an important role for such a transient. The void fraction comparisons indicate that there is still room for improvement of the HRM model.
- For the wall friction model, there is quasi no difference between the FRM model and the steady state friction model which means that the wall friction is not an important factor for such a transient, or that it provides insufficient damping.

6. Conclusions

The wall shear stress at the wall has been modeled for fast transient flows resulting from the fast closure of a valve. It is shown that the wall shear stress evolution involves two steps: the first step corresponds to a sudden change of the wall shear stress for each passage of the pressure wave, the second step is a relaxation process of the wall shear stress to the steady state flow conditions. The model is described by Eq. (6) and is called ''Friction Relaxation Model''. This model was implemented in the WAHA code.

The WAHA code developed during the WAHALoads project in the frame of the Fifth European Program is based on a 6-equation two-fluid model in an elastic pipe with second-order accurate numerics. It allows simulations of ideal gas–liquid water mixtures, or vapour–liquid water mixtures. The geometry consists of a set of pipes with smooth varying cross-sections, or abrupt area changes. At the boundaries closed ends, constant pressure tanks or constant velocity can be considered. The model is made more realistic by including relaxation models for the simulation of the non-equilibrium phenomena encountered in fast transients.

The WAHA code has been tested against several test cases. In this paper, three test cases have been chosen for verification of the ability of the WAHA code to correctly predict fast transient two-phase flow. The results of the WAHA code simulations are more or less in good agreement with the data of the test cases. Nevertheless further improvements are still needed to better simulate ''cavitation'' water hammers.

Acknowledgement

This work has been done in the frame of the WAHALoads project (FIKS-CT-2000-00106) of the Fifth Framework Programme sponsored by the European Commission. The authors acknowledge Prof. G. Winckelmans from UCL and Prof. H. Lemonnier from CEA for usefull discussions on the Friction Relaxation Model.

References

Bilicki, Z., Giot, M., Kwidzynski, R., 2002. Fundamentals of two-phase flow by the method of irreversible thermodynamics. Int. J. Multiphase Flow 28 (12), 1983–2005.

Downar-Zapolski, P., Bilicki, Z., Bolle, L., Franco, J., 1996. The non-equilibrium relaxation model for one-dimensional flashing liquid flow. Int. J. Multiphase Flow 22 (3), 473–483.

Dudlik, A., 2003. Data Evaluation Report on PPP water hammer tests, cavitation caused by rapid valve closing, WAHALoads report, Deliverable D35, Revision June, 2003, Fraunhofer Institut Umwelt-, Siecherheits-, Energietechnik UMSICHT.

Haar, L., Gallagher, J.S., Kell, G.S., 1984. NBS/NRC Steam Tables Thermodynamic and Transport Properties and Computer Programs for Vapor and Liquid States of Water in SI units. Hemisphere Publishing Corp., New York, 320 pp.

Holmboe, E.L., Rouleau, W.T., 1967. The effect of viscous shear stress on transients in liquid lines. Transactions of ASME, Journal of Basic Engineering, 174–180.

Jou, D., Casas-Vasquez, J., Lebon, G., 2001. Extended Irreversible Thermodynamics. Spinger-Verlag, Berlin, Heidelberg.

Kucienska, B., 2004. Friction Relaxation Model for Fast Transient Flow. Université catholique de Louvain (UCL). Doctoral thesis.

Kucienska, B., Seynhaeve, J.M., Giot, M., 2002. Use of extended irreversible thermodynamics to predict transient dissipative effects with the HEM and HRM models. In: 40th European Two-Phase Flow Group Meeting in Stockholm and 2nd European Multiphase Systems Institute Meeting, 10–13 June 2002.

Lemmonier, H., 2002. An attempt to apply the homogeneous relaxation model to the WAHALoads benchmark tests with interaction with the mechanical structure. CEA-T3.3-D61-200302, WAHALoads project deliverable D61.

Mills, A.F., 1999. Heat transfer, second ed. Prentice-Hall.

Pezzinga, G., 1999. Quasi 2D model for unsteady flow in pipe networks. Journal of Hydraulic Engineering 125 (7), 676–685.

Rousseau, J.C., 1986. Experimental data sets for evaluation of modelling methods (HEWITT G.F. Harwell Laboratory). Data set No 13.

Simpson, A.R., 1986. Large water hammer pressure due to column separation in sloping pipes (transient cavitation). PhD thesis. University of Michigan.

Tiselj, I., Horvat, A., 2002. Accuracy of the operator splitting technique for two-phase flow with stiff source terms. Proceedings of ASME Joint U.S.–European Fluids Engineering Conference, July 14–18, 2002. Montreal.

Tiselj, I., Petelin, S., 1997. Modelling of two-phase flow with second-order accurate scheme. Journal of Computational Physics 136 (2), 503–521.

Tiselj, I., Horvat, A., Černe, G., Gale, J., Parzer, I., Mavko, B., Giot, M., Seynhaeve, J.M., Kucienska, B., Lemonnier, H., 2004. WAHA3 code manual, Final report of the WAHALoads project, EU 6th program (FIKS-CT-2000-00106).

Vardy, A.E., Hang, K., 1991. A characteristic model of transient friction in pipes. Journal of Hydraulic Research, IAHR 29 (5), 669–684.